Photosensitive vesicles from a *cis*-azobenzene gemini surfactant show high photoresponse†‡

Rony Kiagus Ahmad,[a] Delphine Faure,[a,b] Pascale Goddard,[b] Reiko Oda*[a] and Dario M. Bassani*[b]

Received 4th March 2009, Accepted 6th May 2009
First published as an Advance Article on the web 8th June 2009
DOI: 10.1039/b904390j

A zwitterionic gemini surfactant containing a photoactive azobenzene chromophore forms vesicles in aqueous solution only from a photostationary state containing a majority of the *Z*-isomer (26:74 *E*:*Z*). These vesicles are stable in the dark over several weeks, trapping the azobenzene in the Z form. Compared to an analogous system based on a cationic azobenzene gemini surfactant forming vesicles with the *E*- but not the *Z*- isomer, the new system displays significantly enhanced photosensitivity towards light-induced lysis of the vesicles.

Introduction

Amphiphilic molecules bearing chromophores capable of undergoing photoinduced isomerization, polymerization or lysis form photoresponsive supramolecular systems[1] in which properties such as viscosity, micellization, sol-gel transition, or the disruption of vesicles, can be controlled.[2] Whilst the popularity of azobenzene chromophores in the design of photochromic systems rests on their proven reversible photochromic response and relative synthetic accessibility, photocontrol based on the photoinduced scission of the amphiphilic moiety tends to show better photoresponse.[3–6] With some exceptions,[7] examples of photocontrol of surfactant aggregates based on photoisomerization generally show only modest response upon irradiation. Furthermore, the structural changes thus induced are generally tolerated by the dynamic amphiphilic architecture unless the latter has strong local ordering (*e.g.* crystals or organized in two dimensional films).[3,1h,i,k]

We recently reported an amphiphilic system based on a cationic gemini surfactant incorporating an azobenzene scaffold.[8] Compared to related stilbene chromophores, azobenzenes possess accrued photostability and better resolved absorption bands of the *E* and *Z* isomers, making them preferred in applications targeting reversible photocontrol of chemical properties.§ Photoinduced $E \rightarrow Z$ isomerization of **1** (Scheme 1) is proposed to alter the occupational area of the head *vs.* tail groups and was shown to provoke reversible light-induced variations in the surface pressure of monolayers of **1** at the air-water interface. The system was designed to exploit the photochemical stability of azobenzene isomerization while maintaining the chromophore parallel to the interface, thus ensuring sufficient space for isomerization. Despite this, vesicles of **1** in water are stable to irradiation unless a small amount of CTAB is present. The latter destabilizes the vesicles and pre-disposes them to undergo light-induced lysis, albeit inefficiently. In this respect, **1** behaves similarly to other light-sensitive systems based on *E, Z* isomerization that have been reported previously, requiring long irradiation times and/or high power sources. We now report a zwitterionic system (compound **2**, Scheme 1) in which the azobenzene chromophore is activated by pre-irradiation to form the thermodynamically unfavorable *Z* isomer. In the dark, the latter is relatively long-lived and allows further transformations of the sample. Vesicles prepared from these samples are stable over several weeks in the dark, but undergo light-induces lysis even at low light intensities.

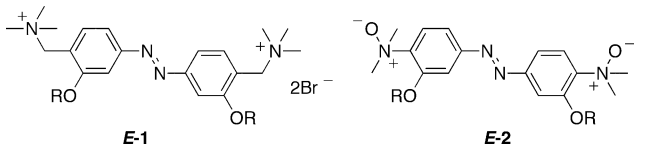

Scheme 1 Cationic and zwitterionic gemini surfactants possessing an azobenzene spacer.

Results and discussion

The structures of **1** and **2** (Scheme 1) are based on the use of a photoactive azobenzene chromophore as a rigid scaffold to connect two alkylammonium amphiphiles. Molecular modeling of the *E* and *Z* conformers suggests that isomerization of the N=N double bond will significantly alter the relative area occupied by the polar head groups with respect to the non-polar alkyl chains. Additionally, whereas conformer *E* is expected to be near-planar, the *Z* isomer is significantly distorted because of non-bonded repulsions between the alkoxy substituents. It is therefore anticipated that upon photo- or thermal *E, Z* isomerization, the ensuing structural variation will induce an important reorganization of the surfactant aggregates.

Compounds **1** and **2** were prepared from 2-methyl-4-nitrophenol and 2-amino-4-nitrophenol, respectively, by reductive

[a]*Institut Européen de Chimie et Biologie, CNRS UMR CBMN-5248, 2 rue Robert Escarpit, 33607, Pessac, France. E-mail: r.oda@iecb.u-bordeaux.fr; Fax: 335 4000 3066; Tel: 335 4000 2229*
[b]*Institut des Sciences Moléculaires, CNRS UMR 5255, 33405, Talence, France. E-mail: d.bassani@ism.u-bordeaux1.fr.; Fax: 335 4000 6158; Tel: 335 4000 2827*

† Dedicated to Pr. Shinkai on the occasion of his 65th birthday.

‡ Electronic supplementary information (ESI) available: ^{1}H and ^{13}C NMR of **1** and **2**, ms of photolyzed samples of **2**, UV-VIS absorption spectra of **1** and **2** in dichloromethane solutions at different irradiation times. See DOI: 10.1039/b904390j

§ Surfactants containing photo-isomerisable stilbene units have been reported to undergo micelle to vesicle transition,[3] but stilbene photoisomerisation exhibits significant photochemical fatigue because of competitive photocyclisation from the *Z*-isomer to afford dihydrophenanthrene.

coupling according to Scheme 2. Alkylation of the phenol group under mildly basic conditions smoothly introduced the hydrocarbon chains. Following reductive coupling using $LiAlH_4$ in THF, quaternization of the corresponding tertiary amines was attempted as an entryway to the corresponding bis-cationic azo-amphiphiles. In contrast to **1**, where bis-cationization is achieved from the corresponding bromomethyl derivative **5** using an excess of trimethylamine, reaction of **10** with an excess of iodomethane only affords the mono-cationic intermediate. More vigorous conditions or alkylating reagents (*e.g.* dimethylsulfate) lead to decomposition. Fortunately, oxidation of the aromatic amines in **10** with *m*-CPBA proved successful and led to the amine-oxide amphiphile **2**. Both **1** (with bromide counterions) and **2** are soluble in chloroform, but form aggregates in aqueous environments.

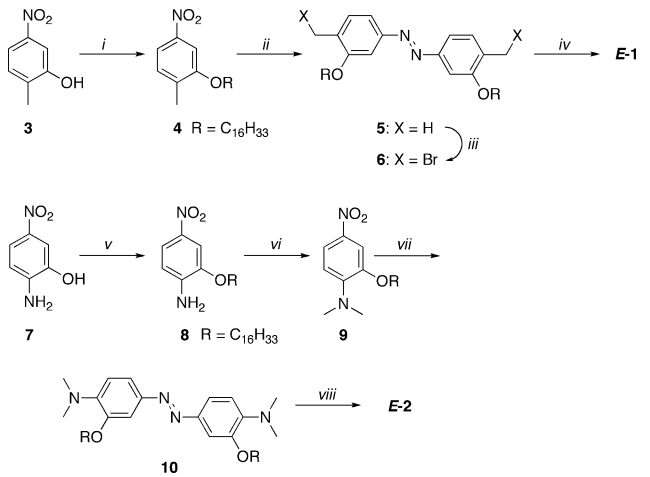

Scheme 2 Syntheses of *E*-**1** and *E*-**2**. *i*, $C_{16}H_{33}I$, K_2CO_3 18-*crown*-6, THF, 80 °C (95%); *ii*, $LiAlH_4$, THF, 80 °C (33%); *iii*, NBS, CCl_4, reflux (50%); *iv*, Me_3N, CH_3CN, 20 °C (90%); *v*, $C_{16}H_{33}I$, K_2CO_3 18-*crown*-6, THF, 80 °C (95%); *vi*, MeI, DMF, 90 °C, (40%); *vii*, $LiAlH_4$, THF, 80 °C (30%); *viii*, *m*-CPBA, $CHCl_3$, −5 °C (20%).

The UV-Vis electronic absorption spectra of *E*-**1** and *E*-**2** in chloroform are typical of azobenzene derivatives, exhibiting strong π–π* absorption bands centered around 300 nm and a weaker n–π* transition located at *ca.* 450 nm (Fig. 1). To elucidate the origin of the shoulder at 350 nm in the absorption spectra of *E*-**1**, we performed INDO/S SCF-CI calculations (ZINDO) on the PM3-optimized geometry. The results show that in **1**, the π–π* HOMO–LUMO transition typical of azobenzenes is accompanied by an additional π–π* transition originating from mixing of the HOMO-2-LUMO transition with the HOMO–LUMO transition. Compared to **1**, **2** possesses electronic transitions that are shifted bathochromically, a consequence of the inductive electron withdrawing *vs.* donating effect of the ammonium *vs.* methylene substituents.

As typically observed for azobenzene derivatives, irradiation of *E*-**1** and *E*-**2** at 365 nm leads to the isomerization of the azo bond to afford photostationary states (PSS) that are enriched in the *Z* isomers. In dichloromethane, the isomerization occurs cleanly, giving rise to isosbestic points at 410 nm and 394 nm for **1** and **2**, respectively. The composition of the PSS can be readily determined by ^{1}H-NMR spectroscopy, as the two isomers exhibit well-resolved spectra that are significantly shifted (see experimental section). This information can then be used to deduce the absorption

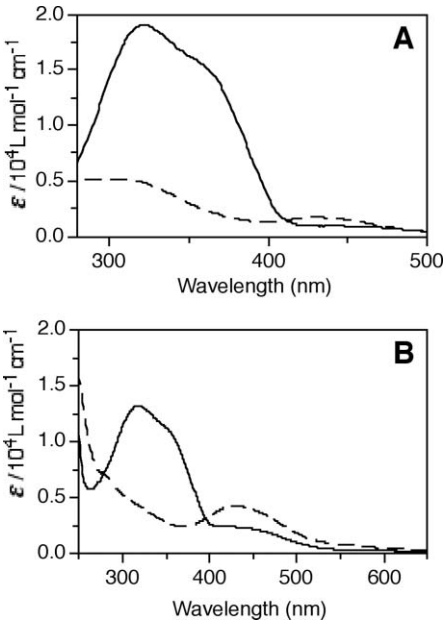

Fig. 1 Electronic absorption spectra of the *E* (solid lines) and *Z* isomers (dashed lines) of **1** (A) and **2** (B) in dichloromethane.

spectra of the *Z* isomers reported in Fig. 1. The composition of the PSS at 365 nm and 450 nm, and the calculated extinction coefficients at λ_{max} for the *E*- and *Z*-isomers of **1** and **2** are given in Table 1. Overall, the compounds behave similarly with the notable exception that the rate of thermal $Z \rightarrow E$ isomerization of **2** is considerably slower (by a factor of three) than that of **1** ($t_{1/2} = 4.8$ and 14.8 hrs. for *Z*-**1** and *Z*-**2**, respectively). As expected, the return of the *Z* isomer to the *E* form can be accelerated by irradiation with 254 or 450 nm light.

The critical micelle concentrations (CMC) obtained by conductivity and tensiometric measurements are very low for both *E*-**1** and *E*-**2** (CMC = 2.5×10^{-6} M for *E*-**1**, no value could be determined for *E*-**2** due to its low water solubility). In the case of **1**, previous results showed that at concentrations above the CMC, *E*-**1** readily forms vesicular aggregates in aqueous solutions. Vesicles of *E*-**1** containing 10% CTAB were shown to undergo light-induced collapse to a suspension of small crystallites.[8a] Irradiation of monolayers of **1** formed at the air-water interface indicates that an increase in the molar surface area (determined from the minimum area before collapse in π-A isotherms) accompanies $E \rightarrow Z$ isomerization, consistent with the hypothesis that the *Z*-isomer is non-planar and may not pack as well as the *E* isomer. The situation is apparently similar for **2**, which also shows

Table 1 Spectral and photochemical data for **1** and **2**[a]

	λ_{max} (ε)[b]		PSS (*Z*:*E*)[c]		
	E	*Z*	365 nm	450 nm	k_r (s^{-1})[d]
1	325 (18780) 460 (1490)	425 (2760)	80:20	21:79	4.0×10^{-5}
2	316 (13160)	277 (7250)	74:26	16:84	1.3×10^{-5}
	430 (1560)	430 (4280)			2.3×10^{-6}[e]

[a] In dichloromethane. [b] Absorption maxima (nm) and molar extinction coefficient (L mol^{-1} cm^{-1}). [c] Composition of photostationary state. [d] Rate constant for thermal $Z \rightarrow E$ isomerization in the dark at 20 °C. [e] Thermal isomerization in aqueous vesicles determined from Fig. 4.

an increase in molar surface area upon photoinduced $E \rightarrow Z$ isomerization (Fig. 2), although the light-induced increase in the molar surface area is significantly smaller than for **1**. Indeed, as the PPS is reached upon irradiation with 365 nm light, the molar surface area at surface pressure 41 mN/m is observed to increase from 50 or 56 Å^2/molecule to 70 or 64 Å^2/molecule, for **1** or **2**, respectively. A possible explanation for the smaller variation in the case of **2** is that, compared to the di-cationic nature of **1**, the zwitterionic nature of **2** reduces the Coulombic repulsion between molecules.

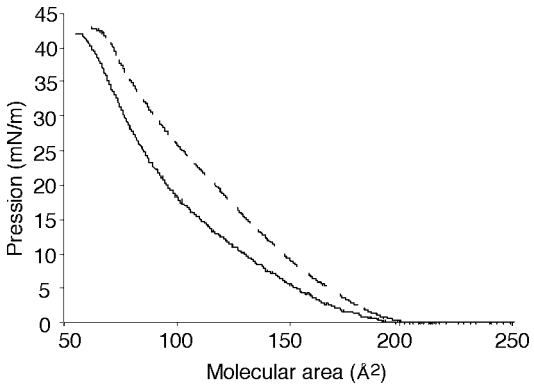

Fig. 2 Effect of 365 nm irradiation on π-A isotherms of **2** at the air-water interface. Solid line: *E*-**2**. Dashed line: PSS(365 nm) mixture of *E*- and *Z*-**2** obtained by pre-irradiation of the sample prior to deposition.

A striking difference between **1** and **2** is the relative dispersibility of the *Z* and *E* isomers, which leads to widely divergent behavior of the aggregates towards irradiation. For **1**, the *E* isomer can easily form aggregates in water, and irradiation of these aggregates in water leads to the formation of a precipitate. In the case of **2**, the low water solubility of the *E* isomer prevents it from forming solutions of dispersed aggregates under conditions that are conducive for the formation of vesicles from *E*-**1** (sonication and gentle heating). However, the significant thermal stability of the *Z* isomer of **2** allowed us to envisage formation of vesicles from the *E*, *Z* mixture of isomers present in the PSS obtained by irradiation of solutions of *E*-**2** in dichloromethane. Thus, irradiation with 365 nm light followed by evaporation of the organic solvent affords a powder that is readily solubilized in water. The composition of the sample thus obtained is close to the proportion of *Z* and *E* isomers characteristic of the initial PSS ($Z/E = 74/26$, Table 1), as verified by its absorption spectra. To confirm and better quantify the higher solubility of the irradiated sample, the Krafft temperatures of the irradiated and non-irradiated samples were determined at two concentrations (Table 2). In both cases, the Krafft temperature of the irradiated sample is lower than that of the non-irradiated sample (*E*-**2**). Importantly, at concentrations of 0.6 mM, *E*-**2** is insoluble in water up to temperatures of *ca.* 100 °C, whereas samples of **2** enriched in the *Z* isomer are solubilized at only 40 °C. This has a profound impact on the aggregation properties of **2**, as only samples prepared from the PPS(365 nm) mixture of *Z* and *E* isomers lead to the formation of solubilized aggregates in water.

The nature of the aggregates formed upon solubilization of the PSS(365 nm) mixture of irradiated samples of **2** was explored using optical microscopy with differential interferential contrast

Table 2 Krafft temperature of **2**[a]

	100 μM	600 μM
E-**2**	55 °C	98 °C
PSS (365 nm)	32 °C	40 °C

[a] In aqueous solutions.

(DIC). The images are very similar to those previously obtained for *E*-**1**, for which the presence of vesicles that are polydisperse in size, ranging from a few hundred nm to ~10 μm was evidenced by freeze fracture transmission electron microscopy (FFTEM). Fig. 3 shows the difference between the globular, polycrystalline aggregates formed by *E*-**2** *vs.* the vesicular aggregates obtained by solubilization of the PSS(365 nm) mixture of **2**. In this respect, **2** behaves contrary to **1**, which only forms vesicles from the *E* isomer, and for which irradiation of the aggregates in water leads to precipitation. The specific reasons behind this contradictory behavior presumably lie in the subtle balance between the solid-state crystal packing forces and the hydrophilicity of the polar head groups in the *E* and *Z* isomers of **1** and **2**. Differences in solubility between the *E* and *Z* isomers of azobenzene-containing polymers are common, and have been attributed to differences in the dipole moment between the isomers.[9]

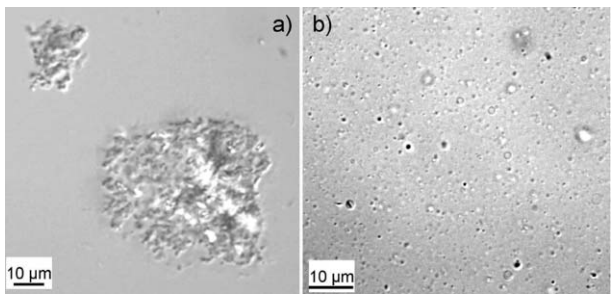

Fig. 3 Optical microscope images of aggregates formed by 5mM dispersions of compound **2** in water. a) E-2; b) PSS(365 nm) mixture of **2**.

As mentioned in the introduction, the vesicular aggregates formed by the solubilization of PSS(365 nm) mixtures of **2** in water are stable over several weeks in the dark. To investigate this point further, we proceeded to follow the evolution of solutions of the vesicles formed from PSS(365 nm) mixtures of **2** (5 mM in water) by optical microscopy and by UV-Vis absorption spectroscopy. The latter allows evaluation of the composition in *E* and *Z* isomers based on the strong absorbance of the transition at 315 nm present in *E* isomer. To improve reproducibility and to minimize scattering from inhomogeneous or highly absorbing samples, aliquots of the 5 mM aqueous solution of the aggregates were diluted to 200 μM just prior to recording the absorption spectra. At $t = 0$, the absorption spectra (Fig. 4a) is similar to that of the PSS mixture in dichloromethane. Its slow evolution over several days in the dark is characteristic of thermal $Z \rightarrow E$ isomerization. From the time-dependence of the peak at 316 nm (Fig. 4b), a lifetime for *Z*-**2** in the aggregates of 120 hrs (5 days) can be estimated. However, even after 35 days, the system has not fully reverted to the *E* form, as attested by its UV-absorption spectrum.¶ This implies

¶ The exact composition of the mixture cannot be accurately determined from the absorption spectra.

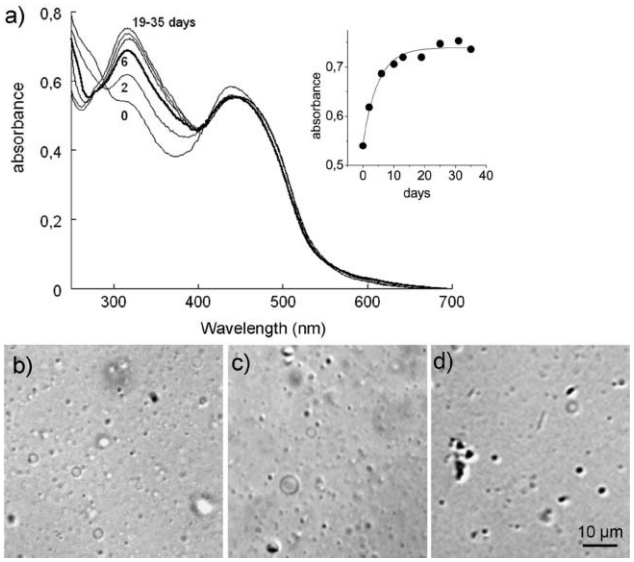

Fig. 4 Evolution of aggregates formed by dispersion of PSS(365 nm) mixtures of 2 (5mM) in water over time in the absence of light. a) UV-Vis absorption spectra (aliquots diluted to 200 μM); inset: Absorbance at 316 nm, solid line represents best fit to monoexponential decay ($k = 2.3 \times 10^{-6}$ s^{-1}). Optical microscope images at $t = 0$ (b), 6 (c), and 24 (d) days.

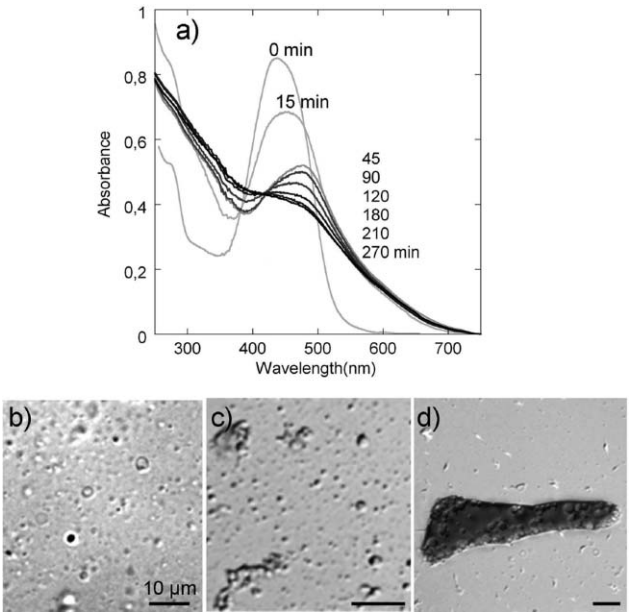

Fig. 5 Vesicles formed from a PSS(365 nm) mixture of **2** (5 mM in water) were irradiated with a low-pressure Hg (254 nm, 7 W). Variation of UV absorption spectra of **2** (a) and optical microscope images of the aggregates following irradiation for 30 (b), 90 (c), and 150 (d) min.

that only a portion of the *Z*-**2** in the aggregates can undergo thermal return to the *E* isomer, whereas the remainder is blocked in the *Z* configuration. The portion that does undergo thermal return does so much more slowly than in fluid solution, where the half-life of the *Z*-**2** isomer is less than one day. The decay of the vesicle population, as judged from the optical microscope images (Fig. 4b-d) is much slower than the thermal isomerization. After 6 days, when the composition of **2** begins to plateau, the samples are still almost exclusively composed of vesicles. Indeed, vesicles persist on timescales of the order of 2–3 weeks, implying that the *Z* and *E* isomers of **2** are trapped in the bilayers of the vesicles. Thus, although *E*-**2** does not possess sufficient solubility to allow the direct formation of vesicles in water, it is possible to circumvent this limitation by irradiation to form a mixture enriched in the more soluble *Z*-**2** isomer.

Irradiation of the vesicles with 450 or 254 nm light accelerates the return to the *E* isomer. Contrary to thermal $Z \rightarrow E$ isomerization, photoinduced isomerization leads to the rapid rupture of the vesicles. This is illustrated in Fig. 5, where the lysis of the vesicles is complete after just 2.5 hrs irradiation with a small (6 W) low-pressure Hg lamp (254 nm) on the solutions in 1 cm quartz cell. For comparison, vesicles formed by related *E*-**1** do not undergo photoinduced lysis unless a small amount of CTAB is added to destabilize them and, even so, require the focused output of a 100 W high-pressure Hg lamp on the solution confined between a slide glass and a cover glass (sample thickness of ~100 μm). As discussed above, the changes in the absorption spectra recorded following irradiation of the aggregates do not match the spectra of *E*-**2** in fluid solution. In fact, the deviation is even more apparent in Fig. 5a, where the decrease in the long wavelength transition is not accompanied by an increase of the band at 320 nm typical of the *E* isomer. Instead, the band at 430 nm undergoes a bathochromic shift of *ca.* 40 nm before decreasing monotonously with an isosbestic point at 410 nm. The absence of an isosbestic point at early irradiation times is synonymous with the occurrence of processes that cannot be modelled by a simple transition between two states. This is presumably due to the aggregation properties of **2**, as mass-spectrometric analysis of the samples after irradiation confirmed that **2** did not undergo decomposition (see ESI‡). The accrued photoresponse of **2** *vs.* **1** may lie in the fact that the vesicles are initially formed from the less stable *Z* isomer, whose return to the more stable *E* form is thermodynamically favored. Additionally, while all vesicles are inherently meta-stable, it is possible that the presence of a high proportion of the insoluble *E*-**2** isomer may further de-stabilize vesicles formed from **2**. In this case, the low cmc of **2** can be an important factor in controlling the stability of the vesicles in that it will slow equilibration *via* the aqueous phase.

Experimental

Reagents and solvents were used as received unless otherwise noted. Tetrahydrofuran was dried over Na/benzophenone and distilled immediately prior to use. Water (18.2 MΩ.cm) was purified on Purelab Prima Elga apparatus. Merck silica gel 60 (70–230 mesh) was used for chromatography. Lyophilization was performed on Heto DryWinner 6–85. Merck silica gel 60 (70–230 mesh) was used for chromatography. ^{1}H NMR and ^{13}C NMR spectra were recorded on a Bruker DPS-200 FT, AC-250 FT or DPX-300 FT spectrometer using deuterium solvent as internal reference unless otherwise indicated. Chemical shifts are given in ppm (δ) with respect to tetramethylsilane. Abbreviations used are s = singlet, d = doublet, t = triplet, q = quartet, and br = broad. Melting points are uncorrected. Mass spectra were recorded on a VG Autospec-Q by EI (70 eV); m/z (%).

Optical Microscopy with Differential Interferential Contrast (DIC): Samples sealed between slide glass and cover glass were observed with a NIKON Eclipse PhysioStation E600FN with adequate condensers and prism for DIC observations.

Krafft Temperatures (*T*k): The Krafft temperature is the minimum temperature at which the hydrated surfactant becomes soluble. Below *T*k, a precipitate is formed. Since the solubilization kinetics is strongly influenced by the presence of any metastable or kinetically controlled aggregates, care was taken so that all samples were treated in the same manner. The powder of surfactant was first solubilized in water to obtain the solution of about 1% w/w, and then it was freeze-dried to get a very fine airy powder. This powder was again dispersed in water to obtain 3 mM solutions, much above the cmc of all the investigated surfactants. To make sure that all the samples formed well-hydrated precipitate, the solutions were plunged into liquid nitrogen to get fast precipitation and freezing, and then they were kept at 2 °C for several hours so that they melted. The temperature of the solutions was increased between 2 and 80 °C with a temperature increase rate of 1 °C per 10 min and the macroscopic aspect was observed. Because **2** is zwitterionic, commonly used conductivity measurements to determine *T*k could not be used.

Kinetics of Vesicles solutions in water without irradiation in dark: Vesicles of the mixture of irradiated samples of **2** were spontaneously formed by dispersing the irradiated (in CH_2Cl_2) and dried powder in water followed by weak sonication (20 seconds in bath type sonicator). Since it was difficult to identify vesicles in the solutions with too low concentration, 5 mM solutions were chosen for kinetics measurements. These solutions were diluted to 200 μM just before UV measurements. Irradiations were conducted with a low pressure mercury lamp (6 W) or with a 365 nm fluorescent lamp (Vilber-Lormat T-6L, 6 W). Actual radiated power was measured with a calibrated NIST-traceable radiometer/photometer to be 2.6 and 4.8 mW/cm^2 at 254 and 365 nm, respectively.

The absorption spectra of **1** and **2** were calculated using INDO/SCF-CI as parametrized by Zerner (ZINDO) at the PM3 energy-minimized geometry.[10]

2-Hexadecyloxy-4-nitrotoluene (4)

In a dry round-bottom flask equipped with a magnetic stirrer and a reflux condenser were placed 2-methyl-5-nitrophenol (1 equiv.), K_2CO_3 (5 equiv.), and a catalytic amount of 18-crown-6. Dry THF was added, followed by 1-iodohexadecane (1.1 equiv.) in dry THF. The mixture was refluxed overnight, cooled, poured into water, and extracted with dichloromethane. The combined organic fractions were successively washed with NH_4Cl (aq), water, brine, and dried over $MgSO_4$. The volatile components were separated on a rotary evaporator and the residual solid purified by flash chromatography (diethylether:pentane 1:9) to afford **4** as a pink solid in quantitative yield. ^{1}H NMR ($CDCl_3$): 7.74 (dd, 1H, J_1 = 2.14 Hz, J_2 = 8.24 Hz); 7.63 (d, 1H, J = 2.14 Hz); 7.26 (d, 1H, J = 8.24 Hz); 4.04 (t, 2H, J = 6.41 Hz); 2.3 (s, 3H); 1.84 (q, 2H, J = 6.71 Hz); 1.26 (br, 26H); 0.85 (t, 3H, J = 7.02 Hz). ^{13}C NMR($CDCl_3$):157.39; 147.17; 135.08; 130.35; 115.42; 105.35; 68.57; 29.35; 23.1; 16.63; 11. MS (FAB+) *m/z* (%): 378 (M + 1, 100), 400 (M + Na, 57.77).

3,3′-Bis(hexadecyloxy)-4,4′-bis(methyl)azobenzene (5)

A dry round-bottom flask equipped with a magnetic stirrer and a reflux condenser in which were placed $LiAlH_4$ (5 equiv.) and dry THF was cooled to −80 °C under a nitrogen atmosphere. A solution of **4** in dry THF was added drop-wise, and the mixture was allowed to return to room temperature, then heated to reflux. After 3 days at reflux, the reaction mixture was cooled, carefully quenched by the addition of water, and extracted with dichloromethane. The combined organic fractions were successively washed with NH_4Cl (10%) and water, and then dried over $MgSO_4$. The volatile components were removed on a rotary evaporator and the residual solid purified by flash chromatography (diethylether:pentane 1:9) to afford **5** as a yellow solid in 33% yield. ^{1}H NMR ($CDCl_3$): 7.47 (dd, 1H, J_1 = 1.89 Hz, J_2 = 7.91 Hz); 7.38 (d. 1H, J = 1.89 Hz); 7.27 (d, J = 7.91 Hz); 4.08 (t, 2H, J = 6.41 Hz); 2.3 (s, 3H); 1.84 (q, 2H, J = 6.71 Hz); 1.26 (br, 26H); 0.85 (t, 3H, J = 7.02 Hz1). RMN ^{13}C ($CDCl_3$):159.8; 150.1; 125.6; 130.1; 114.2; 108.3; 72.6; 29.35; 23.1; 16.63; 11.

4,4′-Bis(bromomethyl)-3,3′-bis(hexadecyloxy)azobenzene (6)

In a two-necked round-bottom flask equipped with a magnetic stirrer and a reflux condenser were placed **5** (1 equiv.), *N*-bromosuccinimide (2.5 equiv.), and a catalytic amount of $(PhCO_2)_2$. Carbon tetrachloride was added, and the mixture refluxed under nitrogen for 8 hrs. After cooling, the precipitate was filtered off and washed with CCl_4. The solution was concentrated on a rotary evaporator and the residual solid obtained purified by flash chromatography (diethylether:pentane 1:9) to afford **6** as a yellow solid in 54% yield. ^{1}H NMR ($CDCl_3$): 7.49 (m, 3H); 4.61 (s, 2H); 4.14 (t, 2H, J = 6.4 Hz); 1.84 (q, 2H, J = 6.71 Hz); 1.26 (s, 26H); 0.85 (t, 3H, J = 7.02 Hz). RMN ^{13}C ($CDCl_3$): 157.6; 154.1; 131.8; 129.7; 117.7; 104.2; 69.2; 29.7; 28.4; 22.4; 14.1. MS (FAB+) *m/z* (%): 688.5 (100).

3,3′-Bis(hexadecyloxy)-4,4′-bis(trimethylammonium-methyl)azobenzene dibromide (1)

A solution of **6** (1 equiv.) was dissolved in dry THF in a two-necked round-bottom flask equipped with a magnetic stirrer and a nitrogen inlet. Dry trimethylamine was bubbled trough the solution, which was allowed to stir at rt for 24 hrs. The solvent was removed on a rotary evaporator and the solid dissolved in a minimum amount of chloroform and precipitated by the addition of acetone. The solid was collected, dissolved in pure water, filtered, and lyophilized to afford **1** as a bright yellow solid (mp = 180–182 °C) in 80% yield. ^{1}H NMR ($CDCl_3$): *E*-**1**: 8.05 (d, 1H, J = 8.25 Hz); 7.61 (d, 1H, J = 7.92 Hz); 7.48 (s, 1H); 5.03 (s, 2H); 4.15 (t, 2H, J = 6.39 Hz); 3.47 (s, 9H); 1.84 (q, 2H, J = 6.71 Hz); 1.26 (s, 26H); 0.85 (t, 3H, J = 7.02 Hz), *Z*-**1**: 7.84 (d, 1H, J = 8.25 Hz); 6.93 (s, 1H); 5.78 (d, 1H, J = 7.92 Hz); 4.04 (t, 2H, J = 6.39 Hz); 3.31 (s, 9H); 1.84 (q, 2H, J = 6.71 Hz); 1.26 (s, 26H); 0.85 (t, 3H, J = 7.02 Hz). ^{13}C NMR ($CDCl_3$): 158.9; 155.0; 136.5; 136.5; 119.0; 117.8; 104.6; 63.5; 53.4; 29.7; 22.7; 14.2. IR (cm^{-1}, KBr): 871, 892, 1105, 1262, 1419, 1469, 1604, 2851, 2920. MS-ESI *m/z* (%): 887 (20, $(M - Br^-)^+$), 403 (100, $(M - 2Br^-)^{2+}$). Elemental analysis: Calculated for $C_{52}H_{94}N_4O_2Br_2 \cdot H_2O$ (M = 984 g mol^{-1}):C, 63.41; H, 9.75; N, 5.69; O, 4.87. Found: C, 63.63; H, 9.65; N, 4.73; O, 5.71%.

4-Amino-3-hexadecyloxynitrobenzene (8)

This compound was prepared in 95% yield starting from 2-amino-5-nitrophenol analogously to **4**. ^{1}H-NMR ($CDCl_3$):7.80 (dd, 1H, $J_1 = 2.28$ Hz, $J_2 = 8.67$ Hz); 7.67 (d, 1H, $J = 2.28$ Hz); 6.65 (d, 1H, $J = 8.67$ Hz); 4.09 (t, 2H, $J = 6.39$ Hz); 1.87 (q, 2H, $J = 6.7$ Hz); 1.26 (s, 26H); 0.88 (t, 3H, $J = 0.2$ Hz). ^{13}C-NMR($CDCl_3$):146.3; 139.0; 138.5; 118.9; 111.7; 106.61; 68.9; 31.9; 22.7; 14.1. ESI-MS m/z (%) 379 (100, M + H$^+$).

4-Dimethylamino-3-hexadecyloxynitrobenzene (9)

A round-bottom flask equipped with a magnetic stirrer and fitted with a reflux condenser and a septum is loaded under nitrogen with **8** (0.25 g, 0.66 mmol), K_2CO_3 (0.45 g, 3.3 mmol), a catalytic amount of 18-crown-6, and 15 mL of dry DMF. Methyl iodide (41 µL, 4.0 mmol) is added through the septum and the mixture is heated to 90 °C with stirring for 24 hrs. The DMF is then removed under vacuum and the oily residue is taken up in dichloromethane, washed with water, and dried over $MgSO_4$. The solvents are evaporated on a rotary evaporator and the waxy solid thus obtained is carefully purified by column chromatography (diethylether:pentane 1:9) to afford **9** (0.1 g) as a yellow solid in 40% yield. ^{1}H-NMR ($CDCl_3$): 7.83 (dd, 1H, $J_1 = 2.15$ Hz, $J_2 = 8.85$ Hz); 7.67 (d, 1H, $J = 2.15$ Hz); 6.75 (d, 1H, $J = 8.85$ Hz); 4.05 (t, 2H, $J = 6.40$ Hz); 1.87 (q, 2H, $J = 6.7$ Hz); 1.26 (s, 26H); 0.88 (t, 3H, J = 0.2 Hz). ^{13}C-NMR ($CDCl_3$):144.3; 139.0; 138.5; 118.9; 111.7; 106.6; 68.9; 43.9; 31.9; 22.7; 14.1. SM (FAB+) m/z (%): 407 (M + 1, 100).

4,4′-Bis(dimethylamino)-3,3′-bis(hexadecyloxy)-azobenzene (10)

Compound **10** was obtained analogously to **5** in 30% yield from **9**. ^{1}H-NMR ($CDCl_3$): 7.50 (dd, 1H, $J_1 = 1.85$ Hz, $J_2 = 8.25$ Hz); 7.43 (d, 1H, $J = 1.85$ Hz); 6.95 (d, 1H, $J = 8.25$ Hz); 4.11 (t, 2H, $J = 6.70$ Hz); 1.87 (q, 2H, $J = 6.7$ Hz); 1.26 (s, 26H); 0.88 (t, 3H, $J = 0.2$ Hz). ^{13}C-NMR ($CDCl_3$): 143.7; 142.6; 132.4; 115.2; 114.0; 109.3; 72.3; 43.9; 30.3; 23.1; 14.0.

4,4′-Bis(dimethylamineoxide)-3,3′-bis(hexadecyloxy)-azobenzene (2)

In a two-necked round-bottomed flask fitted with a septum and a nitrogen inlet is placed **10** (1 equiv.) dissolved in $CHCl_3$. The solution is cooled to −5 °C and a solution of *m*-CPBA (2 equiv.) in $CHCl_3$ (also cooled to −5 °C) is added drop-wise through the septum. The reaction is allowed to warm to rt and is stirred is continued for 12 hrs. The volatile components are removed on a rotary evaporator and the residue is taken up in dichloromethane, washed with water, and dried over $MgSO_4$. The solution is concentrated on a rotary evaporator and triturated with pentane. The solid thus obtained is filtered and dried under vacuum to give **2** as a red-brown solid in 20% yield (mp = 158–160 °C). ^{1}H-NMR ($CDCl_3$): *E*-**2**: 9.02 (d, 1H, $J = 8.55$ Hz); 7.73 (dd, 1H, $J_1 = 8.55$ Hz, $J_2 = 1.82$ Hz); 7.51 (d, 1H, $J = 1.82$ Hz); 4.25 (t, 2H, $J = 5$ Hz); 3.73 (s, 6H); 1.94 (q, 2H, $J = 7.3$ Hz); 1.26 (s, 13H); 0.88 (t, 3H, $J = 0.2$ Hz), *Z*-**2**: 8.68 (d, 1H, $J = 8.55$ Hz); 6.66 (d, 1H, $J = 1.82$ Hz); 6.29 (dd, 1H, $J_1 = 8.55$ Hz, $J_2 = 1.82$ Hz); 4.00 (t, 2H, $J = 5$ Hz); 3.61 (s, 6H); 1.94 (q, 2H, $J = 7.3$ Hz); 1.26 (s, 13H); 0.88 (t, 3H, $J = 0.2$ Hz). ^{13}C-NMR ($CDCl_3$): 153; 150; 140; 125; 118; 104; 68,9; 43.0; 30.3; 23.1; 14.0. IR (cm^{-1}, KBr): 537, 660, 863, 997, 1012, 1270, 1405, 1472, 1601, 2852, 2918. MS-TOF m/z (%): 781 (100), 360 (50). Elemental analysis: Calculated for $C_{48}H_{84}N_4O_4{\cdot}2H_20$ (M = 817.2 g mol^{-1}): C, 70.50; H, 10.77; N, 6.85; O, 11.75. Found: C, 71.13; H, 10.41; N, 6.82; O, 9.66%.

Conclusion

We have prepared a zwitterionic gemini surfactant based on a photosensitive azobenzene scaffold that exhibits slow thermally-activated *Z*-*E* isomerization. The latter property has allowed us to prepare vesicles from photostationary mixtures enriched in the more soluble *Z* isomer. In these aggregates, thermal isomerization to the *E* isomer is slow compared to fluid solution. In the absence of light, the vesicles are stable over several weeks, but can be ruptured by irradiation with a low-power lamp.

Acknowledgements

Financial support from the CNRS, the French Ministry of Research and Asian development bank is gratefully acknowledged.

Notes and references

1 (*a*) M. Haubs and H. Ringsdorf, *Angew. Chem. Int. Ed. Engl.*, 1985, **24**, 882; (*b*) I. R. Dunkin, A. Gittinger, D. C. Sherrington and P. J. Wittaker, *J. Chem. Soc. Chem. Commun.*, 1994, 2245; (*c*) Z. Li and A. G. Kutateladze, *J. Org. Chem.*, 2003, **68**, 8236; (*d*) J. Eastoe, M. S. Dominguez, H. Cumber, P. Wyatt and R. K. Heenan, *Langmuir*, 2004, **20**, 1120; (*e*) T. Kunitake, N. Nakashima, M. Shimomura and Y. Okahata, *J.Am. Chem. Soc.*, 1980, **102**, 6642; (*f*) T. Kunitake, Y. Okahata, M. Shimomura, S. Yasunami and K. Takarabe, *J. Am. Chem. Soc.*, 1981, **103**, 5401; (*g*) W. F. Mooney, P. E. Brown, J. C. Russel, S. B. Costa, L. G. Pedersen and D. G. Whitten, *J. Am. Chem. Soc.*, 1984, **106**, 5659; (*h*) D. A. Holden, H. Ringsdorf, V. Deblauwe and G. Smets, *J. Phys.Chem.*, 1984, **88**, 716; (*i*) K. Nishiyama and M. Fujihira, *Chem. Lett.*, 1988, 1257; (*j*) S. D. Evans, S. R. Johnson, H. Ringsdorf, L. M. Williams and H. Wolf, *Langmuir*, 1998, **14**, 6436; (*k*) H. C. Kang, B. M. Lee, J. Yoon and M. Yoon, *J. Colloid Interface Sci.*, 2000, **231**, 255; (*l*) J. Eastoe; and A. Vesperinas, *Soft Matter*, 2005, **1**, 338; (*m*) M. Irie, *AdV. Polym. Sci.*, 1993, **110**, 49–65; (*n*) B. L. Feringa, R. A. Van Delden, N. Koumura and E. L. Geertsema, *Chem.Rev.*, 2000, **100**, 1789.
2 (*a*) C. T. Lee Jr., K. A. Smith and T. A. Hatton, *Macromolecules*, 2004, **37**, 5397; (*b*) K. Murata, M. Aoki, T. Suzuki Takaaki Harada, H. Kawabata, T. Komori, F. Ohseto, K. Ueda and S. Shinkai, *J. Am. Chem. Soc.*, 1994, **116**, 6664; (*c*) M. Ayabe, T. Kishida, N. Fujita, K. Sada and S. Shinkai, *Org. Biomol. Chem.*, 2003, **1**, 2744.
3 (*a*) O. Karthaus, M. Shimomura, M. Hioki, R. Tahara and H. Nakamura, *J. Am. Chem. Soc.*, 1996, **118**, 9174; (*b*) J. Eastoe, M. Sanchez-Dominguez, P. Wyatt, A. Beeby and R. K. Heenan, *Langmuir*, 2002, **18**, 7837.
4 H. Sakai, A. Matsumura, S. Yokoyama, T. Saji and M. Abe, *J. Phys. Chem. B*, 1999, **103**, 10737.
5 Y. Orihara, A. Matsumura, Y. Saito, N. Ogawa, T. Saji, A. Yamaguchi, H. Sakai and M. Abe, *Langmuir*, 2001, **17**, 6072.
6 J. Y. Shin and N. L. Abbott, *Langmuir*, 1999, **15**, 4404.
7 T. Shang Kenneth, A. Smith and T. A. Hatton, *Langmuir*, 2003, **19**, 10764.
8 (*a*) D. Faure, J. Gravier, T. Labrot, B. Desbat, R. Oda and D. M. Bassani, *Chem. Commun.*, 2005, 1167; (*b*) M. Geoffroy, D. Faure, R. Oda, D. M. Bassani and D. Baigl, *ChemBioChem.*, 2008, **9**, 2382.
9 (*a*) M. Irie and H. Tanaka, *Macromolecules*, 1983, **16**, 210; (*b*) F. Ciardelli, O. Pieroni and A. Fissi, *J. Chem. Soc. Chem. Commun.*, 1986, 264; (*c*) R. Kroger, H. Menzel and M. L. Hallensleben, *Macromol. Chem. Phys.*, 1994, **195**, 2291; (*d*) C. T. Lee, K. A. Smith and T. A. Hatton, *Macromolecules*, 2004, **37**, 5397.
10 CaChe (Fujitsu Molecular) software package.

